Materials Characterization 113 (2016) 189–197

Contents lists available at ScienceDirect

Materials Characterization

journal homepage: www.elsevier.com/locate/matchar

Influence of multi-microstructural alterations on tensile property inhomogeneity of 7055 aluminum alloy medium thick plate

H. She [a], D. Shu [a,*], J. Wang [a,b], B.D. Sun [a,b]

[a] Shanghai Key Lab of Advanced High-temperature Materials and Precision Forming, Shanghai Jiao Tong University, Shanghai 200240, China
[b] State Key Laboratory of Metal Matrix Composites, Shanghai Jiao Tong University, Shanghai 200240, China

ARTICLE INFO

Article history:
Received 27 October 2015
Received in revised form 22 January 2016
Accepted 27 January 2016
Available online 28 January 2016

Keywords:
Aluminum alloy
Microstructures
Strength
Precipitates
Textures

ABSTRACT

The microstructure of an aged 7055 aluminum alloy medium thick plate at the center and edge was characterized and its influence on tensile property inhomogeneity through the thickness was investigated. The content of coarse second phases is higher and the size is larger at the center than the edge. The precipitates in grains have smaller sizes and a higher number density at the edge than the center due to macro-segregation in the ingot. A higher fraction of low angle grain boundaries (LAGBs) and a stronger β fiber rolling texture retain at the center owing to prevailed recovery, while more fine recrystallized grains exist and the fractions of Brass and Copper texture components obviously decrease at the edge due to higher degrees of recrystallization. The strength is higher at the center than the edge when loaded along RD and TD, while the strength difference between the edge and the center decreases when loaded along the direction of 45°. Moreover, the strength differences in RD, TD and 45° are higher at the center than the edge. The anisotropy of strength and inhomogeneity through the thickness can be mainly attributed to a stronger β fiber rolling texture at the center.

1. Introduction

The sustained requirement of new and high performance lightweight materials for military and civilian aircraft leads to the development of 2xxx and 7xxx series aluminum alloys [1,2]. 7055-T77 plate attracts considerable attention owing to its excellent combination properties of high strength, fracture toughness and stress corrosion cracking resistance [2]. However, a main concern in applications has been the property inhomogeneity across the plate thickness, which results from microstructure inhomogeneity during solidification and subsequent thermal mechanical processing. There are many factors that may influence the microstructure and property inhomogeneity, including the segregation of alloying elements in casting ingots, dissolution of second phases during heat treatment, nonuniform deformation during rolling, recrystallization and quenching sensitivity [3–7].

Four types of major second phases η($MgZn_2$), T($Al_2Mg_3Zn_3$), S(Al_2CuMg) and θ(Al_2Cu) can form in as-cast microstructures of 7055 aluminum alloy [8–12]. In addition, Al_7Cu_2Fe and Mg_2Si are the two main types of impurity phases [11–13]. The remnant of the coarse primary second phases in the final aged alloy are sites of stress concentration or crack initiation to degrade the plasticity, fracture toughness, fatigue properties and stress corrosion cracking of aluminum alloys [10,14–16].

Precipitate plays an important role on the mechanical properties of 7055 alloy. The influences of aging temperature and time on precipitation behavior and the volume fraction, size and coherency with α-Al matrix of the precipitates were studied in detail, and then the influences on strength, ductility and fatigue crack growth rate have also been reported [17–20]. Quench-induced microstructure inhomogeneities which usually occur in the large-scale products result in property inhomogeneity. Liu et al. [6] reported the precipitates inside grains, grain-boundary precipitates (GBPs) and the precipitate free zones (PFZs) in post-artificial aging varied with different quenching temperatures and times. They proposed that natural aging for a long time prior to artificial aging can induce a larger amount of stable GP-I zones to reduce the hardness inhomogeneity [7]. In addition, a lower quench rate can cause the increase of Zn and Mg contents in GBPs and wider PFZs, which leads to the low exfoliation corrosion resistance [21].

A few researches have also been reported about the texture and recrystallization and their influences on properties of 7055 aluminum alloy. The texture gradient through the thickness of 7055-T7751 plate showed that the β fiber texture was dominant in the center layer, in contrast, shear textures were dominant near the surface [5]. With the increase of hot deformation temperature, the volume fraction of recrystallization grains presented a “fall-rise” pattern. The strength and the elongation had the maximum values when the volume fraction of recrystallization grains reached the minimum value [22].

Although some research works have been done in the coarse second phases, precipitates, textures and recrystallization and their influences on the properties of 7055 aluminum alloy, the influence of combining

---

* Corresponding author.
E-mail address: dshu@sjtu.edu.cn (D. Shu).

http://dx.doi.org/10.1016/j.matchar.2016.01.020

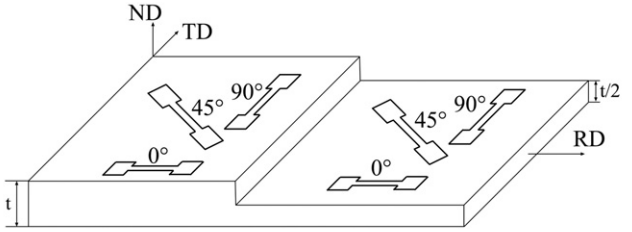

Fig. 1. Scheme of tensile specimens with different angles to the rolling direction.

multi-microstructural alterations during processing on the properties of the plate is seldom reported. In the present paper, the inhomogeneity of microstructures and mechanical properties through the thickness of an aged 7055 aluminum alloy medium thick plate were investigated, and the influences of second phases, precipitates, rolling texture and grain boundaries on the strength and ductility were discussed.

2. Experimental material and procedures

A direct chill casting of 7055 aluminum alloy ingot with a thickness of 520 mm, a width of 1320 mm and a length of more than 3000 mm was used to produce rolling-slab via subsequent thermomechanical treatment of homogenization, hot rolling, solution and artificial aging. The ingot was homogenized at 743 K for 48 h. Before hot rolling, the ingot was scalped and then preheated at 673 K for 1 h. The rolling direction was parallel to the long transverse direction of the ingot. The thickness of the 7055 aluminum alloy ingot was reduced to 27 mm after hot rolling. Finally, the rolling plate was subjected to a complex solution and aging treatment in T7751-like temper.

The chemical compositions of the border and center along the thickness direction of the ingot after homogenization treatment were measured by Direct-reading Spectrometer and the microstructures were observed by optical microscopy (OM) and scanning electron microscopy (SEM). The microstructures of the 7055 plate in T7751-like temper were examined on the RD (rolling direction)–ND (normal direction) plane with the samples cut from the edge and center, respectively. The composition of residual coarse particles in the plate was obtained by energy dispersive spectroscopy (EDS) via SEM and their area fraction and sizes were statistically analyzed over a number of SEM images in backscattering electron (BSE) mode by Digital Micrograph software with mechanically polished samples without etching. Samples for electron back scattered diffraction (EBSD) taken from the plate were prepared by mechanical polishing and then vibratory polished for 2 h. EBSD was performed on an FEI NOVA NanoSEM equipped with a field emission gun (FEG) at an operation voltage of 20 kV. A step size of 0.6 μm was used for the beam scanning. The obtained patterns were post processed by CHANNEL 5-Oxford Instruments software. A JEM transmission electron microscopy (TEM) with FEG operating at 200 kV was used to analyze the precipitates in the aged plate. Samples for TEM observations were prepared by cutting pieces with thickness of ~500 μm and carefully grounding to a thickness of ~100 μm, then punching disks of 3 mm diameter from these pieces. The disks were thinned by twin-jet electropolishing in a solution of 30% nitric acid and 70% methanol at a temperature of −30 °C and a voltage of 13 V. The number density and size parameters of precipitates inside the grains at the edge and the center of the plate were quantitatively measured respectively by a number of TEM bright field images acquired in several different regions using an image analysis software.

Table 1
Chemical compositions at the border and center of 7055 alloy ingot (wt.%).

Positions	Zn	Mg	Cu	Zr	Fe	Si
Border	8.18	1.92	2.08	0.11	0.06	0.04
Center	7.62	1.84	1.95	0.11	0.06	0.04

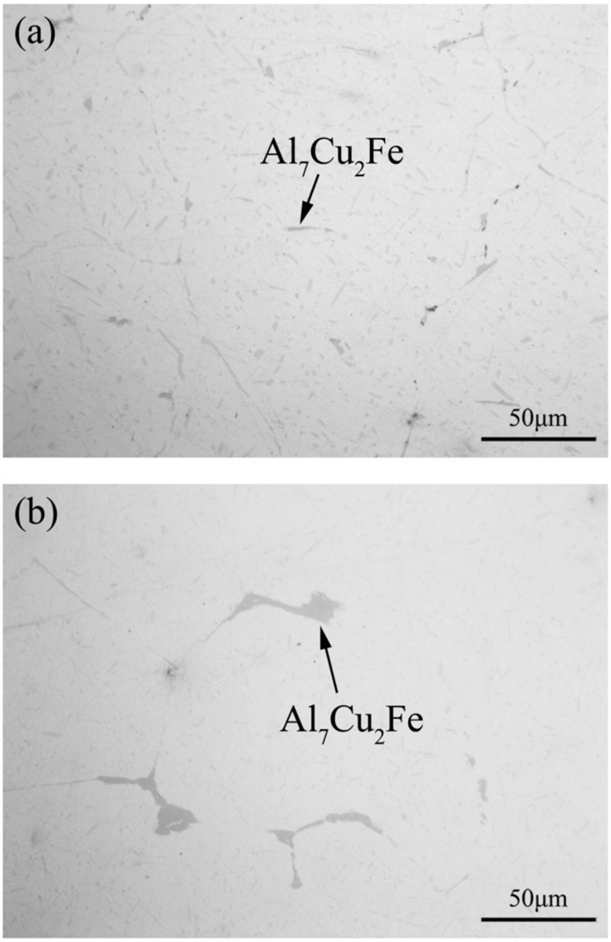

Fig. 2. Al_7Cu_2Fe phase in homogenized 7055 alloy ingot (a) at the border, (b) at the center.

The tensile samples with a 3.5 mm × 2 mm cross-section and a gauge length of 15 mm were machined from the edge and the center of the aged plate in three directions, viz., 0°, 45° and 90° to the rolling direction as shown in Fig. 1. The uniaxial tensile was correspondingly loaded in 0°, 45° and 90° to the rolling direction with a rate of 1 mm/min at ambient.

3. Results

3.1. Chemical and microstructural inhomogeneities of homogenized 7055 alloy ingot

The chemical compositions of the border and the center along the thickness direction of the 7055 alloy ingot after homogenization treatment are shown in Table 1. It shows a visible difference in the content of Zn, Mg and Cu between the border and the center of the ingot due to macro-segregation [23]. The content of Zn, Mg and Cu at the border are respectively 1.07, 1.04 and 1.06 times of that at the center, and the Zn:Mg ratio at the border is 1.03 times of that at the center. Additionally, the content and the size of the coarse Al_7Cu_2Fe phase of the ingot are greater at the center than the border as seen in Fig. 2, which may result from the slower cooling rate at the center of the ingot [23–25].

3.2. Residual coarse phases in the aged plate

In aged 7055 aluminum alloy, there are significant fractions of coarse intermetallic phases that remain undissolved after solution both at the edge and the center of the plate aligned with the rolling direction as shown in Fig. 3. These particles are identified as two kinds of phases